

Individualized targeting and optimization of multi-channel transcranial direct current stimulation in drug-resistant epilepsy

Marios Antonakakis
Institute for Biomagnetism and
Biosignal Analysis
University of Muenster,
Muenster, Germany
marios.antonakakis@uni-muenster.de

Stefan Rampp
Department of Neurosurgery
University Hospital Erlangen
Erlangen, Germany
Stefan.Rampp@uk-erlangen.de

Christoph Kellinghaus
Epilepsy Center Muenster-
Osnabrueck
Department of Neurology
Klinikum Osnabrueck
Osnabrueck, Germany
Christoph.Kellinghaus@klinikum-os.de

Carsten H. Wolters
Institute for Biomagnetism and
Biosignal Analysis,
Otto Creutzfeldt Center for
Cognitive and Behavioral
Neuroscience
University of Muenster
Muenster, Germany
carsten.wolters@uni-muenster.de

Gabriel Moeddel
Epilepsy Center Muenster-
Osnabrueck
Department of Neurology with
Institute of Translational
Neurology – Epileptology
University Hospital Muenster
Muenster, Germany
Gabriel.Moeddel@ukmuenster.de

Abstract— The principle of epilepsy surgery in patients with drug-resistant focal epilepsy is to localize and then to resect the epileptogenic zone. However, epilepsy surgery might not be feasible if a cortical malformation or focal cortical dysplasia (FCD), is located very close to eloquent areas of the brain. Non-invasive brain stimulation is a promising technique for modulating brain activity and may become a neurotherapeutic approach for suppressing long term epileptic seizures. In the present study, we optimize a multi-channel transcranial direct current stimulation (tDCS) montage based on Electro- (EEG) and Magneto-Encephalography (MEG) source analysis for the therapeutic stimulation of a patient with drug-resistant epilepsy due to an FCD located very close to Broca's area. We first construct a realistic volume conductor Finite Element Method (FEM) model of the patient's head, including skull defects, calibrated skull conductivities and white matter conductivity anisotropy. Single modality (EEG or MEG) and combined EEG/MEG (EMEG) source analysis is performed for localizing the irritative zone that caused interictal epileptic discharges (IEDs). We then adopt a novel optimization algorithm, Alternating Direction Method of Multipliers (ADMM), in order to optimize the multichannel tDCS montage for distributing the injected currents in the target brain region. The patient's source analysis indicates localizations on the FCD and orientations to a different cortical side depending on the used measurement modality. The resulting tDCS optimized montage is based on one of those source reconstructions and the occurred stimulation montage is focal over the detected FCD. The combination of individual source analysis for targeting and optimization algorithms for the estimation of a tDCS montage is a promising neurotherapeutic approach of suppressing long term epileptic seizures.

Keywords— focal epilepsy, brain stimulation, EEG, MEG, finite element method

I. INTRODUCTION

In patients with focal epilepsy who do not respond to two or three adequate antiepileptic drugs, epilepsy surgery is the most effective treatment option [1]. The principle of epilepsy surgery is to localize and then resect the epileptogenic zone. However, resection may not be feasible if the epileptogenic zone overlaps with eloquent cortical areas, such as Broca's area. For these patients, transcranial direct current stimulation (tDCS) may become a promising treatment alternative [2, 3]. In the present study, we first investigate the accuracy of source analysis of three different measurement modalities, EEG, MEG and EMEG in a patient with an FCD detected on MRI

as structural correlate (step 1). Then, we show optimized transcranial stimulation montage setups and discuss the possibilities of non-invasive transcranial neurostimulation for the present used epilepsy case who has four skull burr-holes resulting from previous invasive EEG monitoring (step 2).

Non-invasive brain stimulation has emerged as a promising tool for modulating brain activity by either increasing or decreasing cortical excitability [4 – 6]. Several studies suggest that tDCS may become a promising treatment alternative for focal epilepsy in the future [2 – 7]. The basic concept of tDCS is the induction and extraction of direct electric currents. Mostly, two large patch electrodes are used [2]. However, with this approach, modulation of cortical excitability cannot be focused to a given portion of the cortex, because the currents are broadly distributed in the brain. Recently, novel approaches have been proposed for controlling the distribution of the currents based on multi-channel montages [7, 8]. Depending on the region of interest (ROI) and safety constraints, the optimization can lead to a current montage of either focality or intensity which is based on the 10-10 EEG electrode positioning system. In the present study, since we think about frequent stimulations and longer-time applications, we prefer an optimization for focality to avoid stimulation of non-target regions, and this is offered by the ADMM [8].

Individualizing the targeting in tDCS is a vulnerable procedure that may lead to suboptimal stimulation of the target ROI [8]. Single modality EEG/MEG or EMEG source analysis is a promising neuroimaging approach for reconstruction of the underlying brain activity [8, 9]. The reconstructed source contains a location and an orientation that can be used as the individual target for optimizing the multi-channel tDCS montage. Recently, it was shown that both EEG and MEG are sensitive to volume conduction effects [9, 16]. Therefore, the modeling parameters, skull conductivity, and anisotropic white matter need to be properly selected due to the violations that they can cause in the EEG and EMEG source reconstruction [9]. In addition, skull defects distort the EEG signal acquired by overlying electrodes and thereby influence source reconstruction. Skull burr-holes resulting from previous invasive EEG monitoring or epilepsy surgery need to be included in a head model for optimal results [11, 12].

The present study utilizes FEM [9] for modeling the complex geometries and skull defects, and a skull conductivity calibration procedure that enables the combination of EEG and MEG [10, 11]. We model the head volume conductor of the patient through our recently developed module, SIMNEURO [9]. The head model includes six basic compartments (scalp, skull compacta and spongiosa, cerebrospinal fluid, gray and white matter), white matter anisotropy, skull holes, and calibrated skull conductivity. The

concept of sub averaging is applied in the source reconstruction of IEDs for the estimation of the source extend [13]. Finally, an optimized multi-channel montage is presented based on the application of the ADMM algorithm considering as target vector, one of the reconstructed dipoles that are close to the structural lesion (FCD) detected on MRI.

The description of methods and patient's data used is illustrated in Section II. The results of the study are presented in Section III, and followed by a relevant discussion and an outlook in Section IV.

II. MATERIAL AND METHODS

A. Ethical Statement

The patient signed written consent forms, and all procedures have been approved by the ethics committee of the University of Erlangen, Faculty of Medicine on 20.02.2018 (Ref No 4453 B).

B. Clinical Case Description

The patient is a 20-year-old female with epilepsy since the age of 14. Seizure semiology was described as distributed thinking and inability to speak or follow a conversation, without any motor symptoms and without impairment of awareness. The patient did not become seizure free despite treatment with multiple anticonvulsant drugs. Despite her rather mild semiology, the patient felt highly disturbed by her seizures. As she met the criteria for pharmacoresistance, a presurgical evaluation for possible resective epilepsy surgery was done. The first non-invasive video-EEG monitoring showed seizure onset in the left frontal area. MRI imaging in a 3-Tesla scanner including 3D-FLAIR and 3D-T1 was reported as normal, but a FCD-suspect area in the middle frontal gyrus. The fludeoxyglucose positron emission tomography (FDG-PET) showed a slight hypometabolism in the left superior frontal gyrus (Fig. 1a). In an initial EMEG measurement, which was performed on an outpatient basis while the patient was on her antiepileptic medication, no interictal epileptiform discharges (IEDs) occurred. An invasive EEG monitoring was done based on the evidence of the diagnoses described. Four invasive electrodes were implanted in the left frontal lobe (Fig. 1b). Several habitual seizures were recorded, with the implanted electrodes showing typical spread patterns instead of seizure onset patterns. Therefore, no resection was recommended and the electrodes were removed. Instead, several attempts were made to optimize the patient's medication, which were not successful. A year later, another EMEG recording was done, this time on an inpatient basis after stopping her antiepileptic medication. On this occasion, more than one-thousand IEDs were recorded, so that source analysis could be performed.

C. Recording and Procedure

Simultaneous EEG/MEG measurements were acquired with a sampling frequency of 2400 Hz. The EEG system consisted of 80 electrodes while the MEG system (VMS MedTech Ltd) was comprised of 275 third order axial gradiometers. Six measurements in total were acquired. The first measurement was 7 minutes long, and it contained somatosensory evoked potentials and fields (SEP/SEF) for the skull conductivity calibration analysis [8, 9]. The remaining

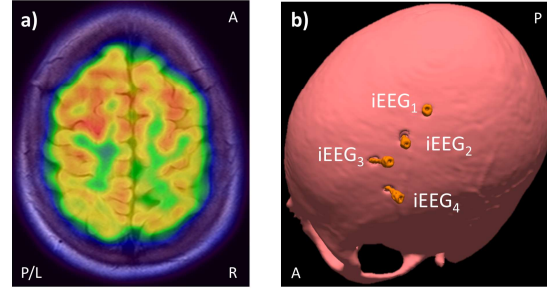


Fig. 1. a) A sagittal slice of fludeoxyglucose positron emission tomography (FDG-PET) that showed a slight hypometabolism in the left superior frontal gyrus, suggesting a possible functional deficit zone; **b)** The reconstructed skull (pink color) with four invasive electrodes – IEEG (namely, IEEG₁, IEEG₂, IEEG₃ and IEEG₄, orange color) were implanted into the suspect deep sulcus and the left superior frontal gyrus (left and middle sketches) and the iEEGs within the skull. The letters, A, P, L and R denote 'anterior', 'posterior', 'left' and 'right' respectively.

five recordings of 8 min duration were measured for the detection of IEDs. The patient was advised to relax and close her eyes during the entire session of the acquisition process.

Structural imaging was done with 3 T MAGNETOM Magnetic Resonance Image - MRI (Siemens Medical Solutions) including T1-weighted (T1w-), T2w-, 3D-FLAIR-T2w- and diffusion-weighted MRI (dMRI) of 1 mm and 1.9 mm resolution, respectively. An additional Computed Tomography (CT, Siemens SOMATOM Definition) set of images, which had been previously been done as part of the invasive EEG procedure, was also used for better delineation of the burr-holes.

During MRI scanning, we placed gadolinium markers at the same nasion, left and right distal outer ear canal positions of the patient for landmark-based registration of EMEG to MRI. All measurements were done in supine position to reduce head movements and to prevent cerebrospinal fluid (CSF) effects due to a brain shift when combining EEG/MEG and MRI [14].

D. Source Analysis

After the bad channels removal, an artifact detection and correction procedure was applied to the patient's EEG and MEG raw data for suppression of the non-cerebral activity [15]. The artifact-reduced data were filtered from 1 to 80 Hz, by using a digital bandpass filter with Hann windowing in CURRY8¹ and a notch filter was applied to reduce the 50 Hz noise component.

Board certified epileptologists marked 1050 spikes with a visible maximum negativity in the EEG at channel F3. The marked spikes were extracted from artifact-reduced portions of the EMEG recording, ensuring that there was no loss of information due to the artifact suppression procedure. The suppressed data was segmented in trials of 200 ms pre- and post- peak of the marked spikes and our spike alignment method [13] in MATLAB (MathWorks, Natick, MA, USA) was performed. With this method, we ensured that all the hand-marked spikes would be at the same propagation phase of the epileptic activity.

Our SIMNEURO pipeline [9] was used for the construction of the realistic volume conductor model and the calibration of the skull conductivity using the somatosensory evoked responses. In particular, the T2w-, 3D-FLAIR T2w-

¹<https://compumedicsneuroscan.com/products/by-name/curry/>

and CT images were first registered to the T1w-MRI, and the construction of a six compartment (skin, skull compacta, skull spongiosa, CSF, gray and white matter) head model was performed based on our recent segmentation module [9]. The four skull holes were hand-segmented using Seg3D², and the dMRI was processed for reducing the eddy currents and susceptibility artifacts [9, 15]. A geometry adapted hexahedral head model was constructed using the SimBio-VGRID [8]. We used standard conductivities for the scalp (0.43 S/m), the CSF (1.79 S/m), and gray matter (0.33 S/m) while the effective medium approach [9] was used for modeling the white matter anisotropy. The skull conductivity was estimated at 0.0041 S/m for skull compacta and 0.01476 S/m for skull spongiosa based on a calibration procedure that involved somatosensory evoked responses source analysis at 20ms post-stimulus, P20/N20 [9, 10]. This calibration procedure contained high signal-to-noise SEP/SEF data and a P20/N20 origin that was mainly tangentially oriented and not too deep [9].

Finally, we performed FEM forward computations based on a fast algebraic multigrid preconditioned conjugate gradient solver using the SimBio³ toolbox. About the source reconstruction, a sub averaging procedure was applied to estimate the centroid and the spread sphere of the irritative zone [10, 13]. The total number of subaverages was 1050, and ten spikes were used per subaverage. Single dipole scans were applied at the onset of each of these subaveraged spikes. Pure MEG source reconstructions were regularized in order to suppress the influence of spatially high frequent data noise that might otherwise be amplified into too high radial dipole orientation components. Before EMEG source analysis, an SNR transformation was applied to both modalities to render them unitless [9].

E. tDCS simulation method

A multi-channel array of 39 possible positions was used for the tDCS optimization of 8 electrodes (Starstim tDCS system, Neuroelectronics, Barcelona, Spain). In order to find the optimum multi-channel tDCS montage for the mainly radially oriented epilepsy target, we utilized the optimization method, ADMM [8]. It is an approach that mainly focuses on the optimization of focal stimulation at the target while reducing the intensity at nontarget regions. The SimBio² toolbox for FEM simulations and MATLAB implementations were used for optimization and visualization.

III. RESULTS

A. Source reconstruction of the epileptic activity

Six “bad” channels (TP9, P6, MLT44, MLT47, MLT55, and MLT56) and ten “bad” epochs were deselected manually through a visual inspection of the raw EEG/MEG data. We then selected 1050 left frontal spikes without any clear artifacts (e.g., eye-blinks) for further analysis. The peak of EEG signal was used as the spike peak. The marked spikes were aligned around the zero-defined line (yellow solid vertical line, Fig. 2) and they were considered as EEG-based IEDs, with maximum negativity at F3 channel (Fig. 2, lower row). Following the previous study [17], we selected the pre spike peak time point, -10.83 ms (Fig. 2, magenta solid vertical line), for rather source analysis at the onset of the spike peak.

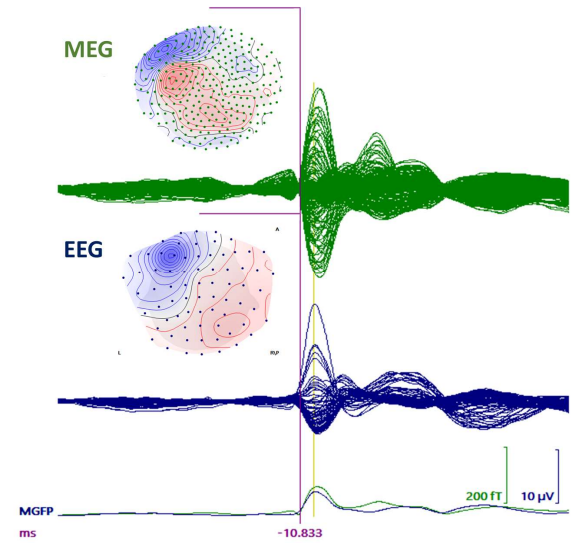


Fig. 2. MEG (upper row) and EEG (lower row) butterfly plots of the averaged spikes (average across all 1050 single epileptic spikes) and scalp topographies are presented. The time point of interest is at -10.83 ms indicated by a solid magenta vertical line. The peak of the grand-average is at 0 ms as indicated by the solid yellow vertical line in the butterfly plots.

A butterfly plot of the averaged 1050 spikes with a scalp topography for MEG (upper part) and EEG (lower part) can be seen in Fig. 2. A clear focal and negative pattern on the EEG scalp topography was presented over the left frontal sensors with maximum negativity at the channel, F3. A dipolar and also rather focal MEG pattern can be observed in the upper part of Fig. 2 which appeared mainly in the frontolateral MEG sensors.

We reconstructed 1050 source dipoles which were estimated by the application of the single dipole deviation scans on each subaverage across ten randomly selected spikes. We ensured that the randomly selected set of ten spikes was unique when compared to other subaverages [10, 13]. The reconstructions of high signal to noise ratio were used for the final estimation of the source centroid and spread sphere for every modality.

Fig. 3 depicts the result of the procedure applied in every modality. About the EEG source reconstruction (blue dipole), the centroid was located in the left inferior frontal sulcus with mainly a radial orientation. The corresponding regularized MEG source reconstruction (green dipole) was slightly more laterally located in a distance of 6.3 mm compared to the EEG dipole. The MEG dipole orientation was perpendicular (90.6°) to the EEG dipole orientation, due to the regularization and the different origin that MEG could detect. Comparing the source strengths, the EEG was 59.2 % higher than the MEG, again due to regularization and different origin. The EMEG source reconstruction (red dipole) was 7 mm and 4.1 mm distant from EEG and MEG, respectively. The EMEG and EEG source orientations were closer (23.4°) than the EMEG and MEG (67.2°), and the source strength was half less for EMEG compared to the EEG (-54 %) than

² <http://www.seg3d.org/>

³ https://www.mrt.uni-jena.de/simbio/index.php/Main_Page

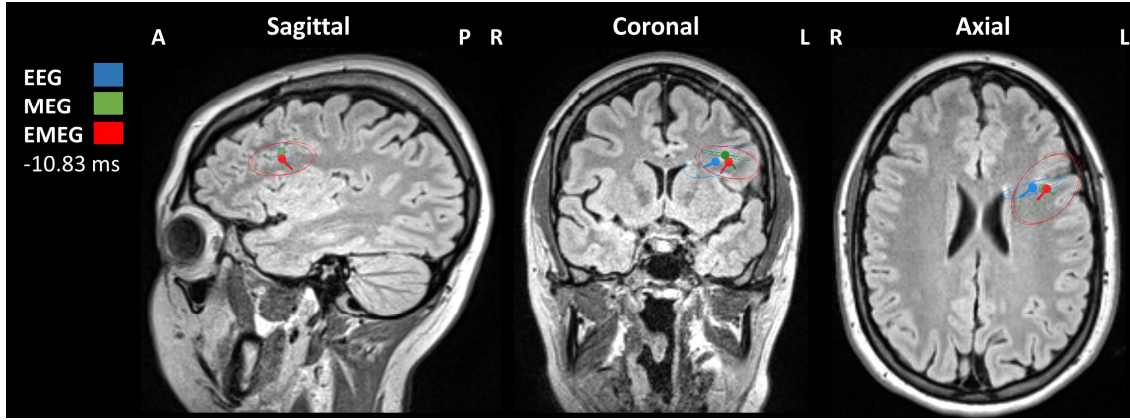


Fig. 3. Spike cluster centroids and spread ellipsoids plotted on the T2w-FLAIR MRI of the patient at the onset of the spike peak (-10.83 ms). The results are presented in blue for EEG, in green for MEG, and in red for EMEG. The letters, A, P, L and R denote 'anterior', 'posterior', 'left' and 'right' respectively.

between EMEG and MEG (37.2 %), most probably due to the insensitivity of the MEG to radial source components. The spread sphere (i.e., source extent) was quite focal for all the reconstructions.

In Fig. 4, the EEG and EMEG source reconstructions and the patient's 3D-FLAIR MRI are illustrated side by side. Compared to MEG, the both EEG and EMEG reconstructed areas at -10.83 ms (Fig.4a) point to detection to a suspect lesion on the MRI (Fig.4b) which is very likely to be a type 2 b focal cortical dysplasia (FCD type 2b) and which was not described earlier by neuroradiological appraisal of the MRI study. The lesion was judged to be in very close proximity to Broca's area, so that a resection would be associated with a high risk of aphasia. Therefore, neurostimulation was considered as an alternative treatment option.

B. The optimized multi-channel tDCS montage

In an application, the EEG source reconstruction was utilized as the target vector (black cone, Fig. 5a) during the optimization of the stimulation montage for multi-channel tDCS. Fig. 5a depicts the simulated tDCS montage as it was estimated by the application of the optimization algorithm. Four highest anodal (FC5, F3, AF3, and AF7) and five lowest cathodal (Fz, C3, T7, F7, and C3) stimulation electrodes occurred after the application of ADMM. The anodal electrodes were mainly in a circle order, and the cathodal electrodes surrounded them. A substantially high focality of the current density distribution was observed over the left middle frontal gyrus with asymmetrical expansions to the surrounded areas (Fig. 5b and c).

Following [8] for the definition of the indices, we also report the intensity in the target region (IT: 0.023 A/m²), the intensity in non-target regions (INT: 0.003 A/m²) and the focality index (FOC = IT/INT: 8) in order to quantify the quality of our tDCS optimization.

IV. DISCUSSION AND OUTLOOK

In the present study, we optimized a multi-channel tDCS montage aiming at the non-invasive individualized transcranial electric stimulation of a patient with drug-resistant epilepsy due to an FCD, who is not a good candidate for epilepsy surgery because of close proximity of the lesion

to Broca's area. While for the targeting, we focused on the part of the irritative zone, to which the EEG and the EMEG was especially sensitive due to the quasi radially orientation of the FCD. For the setup of the head volume conductor model and the calibration of individual skull conductivity for this EEG and EMEG reconstruction, combined SEP/SEF data were used. Out of 1050 recorded spikes, we calculated subaverages that consisted of ten averaged spikes each and used them to calculate centroids and spread spheres as an estimation of source extent. An individualized and realistic head volume conductor model was constructed that included calibrated skull conductivity, the four skull holes from the previous invasive EEG study, and white matter anisotropic conductivity. Source reconstructions were performed utilizing the subaveraging concept for all the measurement modalities. In this first study, we decided to focus on the EEG reconstruction for the targeting process, as together EMEG source reconstruction, they were corresponded best to an FCD-suspect lesion on the FLAIR-MRI. The final step was then the application of the multi-channel tDCS optimization method, ADMM, which resulted in mainly three anodal and five cathodal channels, stimulating quite focally over Broca's area or the left middle frontal gyrus.

All source reconstructions at -10.83 ms before the spike peak of all three modalities were over the left frontal area

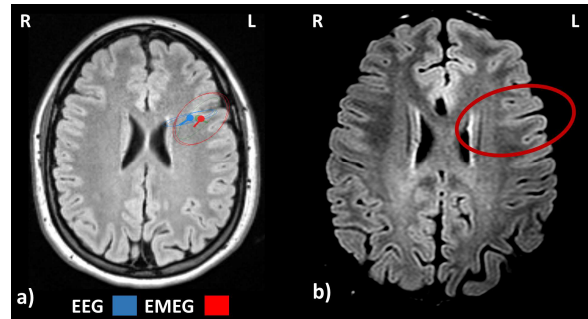


Fig. 4. a) The estimated sources with estimated extent (spread sphere) from EEG and EMEG at -10.83 ms was located in an area where **b)** the patient's 3D-FLAIR MRI was also suspicious with regard to an FCD (see the blurred cortical area in the middle of the red ellipsoid). The letters, L and R denote 'left' and 'right' respectively.

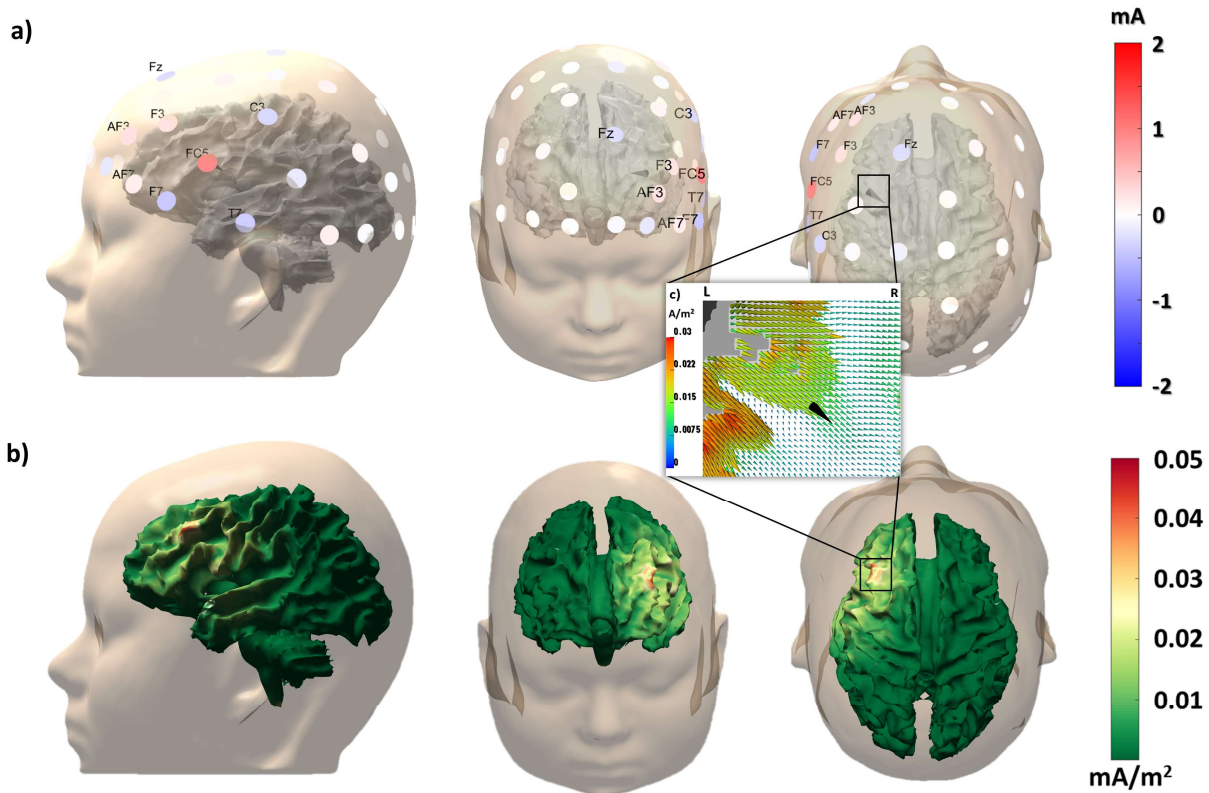


Fig. 5. a) The optimized tDCS montage. The EEG-defined target is indicated as a black cone. **b)** the optimized current density distribution on the patient's cortex and **c)** an axial MRI in zoom-view mode of the optimized currents at the target area. The channels are colored by the optimized currents ranging from -2 up to 2 mA. The total sum of the of the injected currents was equal to 2 mA to fulfill safety constraint. The colored brain surface of the patient represents the distribution of the current density measured in mA/m². The visualization of the sub-pictures a) and b) were created in MATLAB by using our own scripts while the sub-picture c) was visualized by the use of openly available toolbox, Scirun⁴.

(Fig. 4). EMEG and MEG source locations were closer to each other than EMEG and EEG, while EEG and MEG source centroids had a distance of only 6.4 mm to each other. For the source orientation and strength components (dipole moments), an almost similar orientation pattern was observed between EMEG and EEG, while due to (a) regularization, (b) a different origin and (c) the weakness of while MEG dipole orientation was nearly perpendicularly oriented to both EEG and EMEG, due to the same reasoning, EMEG source strengths were much closer to MEG than to EEG. We can thus observe that EMEG location is mainly driven by MEG, while EMEG orientation is mainly influenced by the EEG. Similar results with regard to this complementarity of EEG and MEG were reported in [9, 13].

The EEG and EMEG source centroid and extent at -10.83 ms was localized more caudally and deeper than for MEG. The deep FCD in a sulcal valley, retrospectively found in the 3D Flair-MRI (Fig. 4b), supports this notion and also explains why in this case study, the EEG and EMEG bear the dominant information. From sensitivity investigations [18], it gets clear that the EEG is much more sensitive to deep and radially oriented sources than the MEG. An underlying source in the sulcal valley with its mainly radial orientation is thus one of the few cases where the MEG can not contribute as much as it is normally able to do. Already from the scalp topographies (Fig. 2), we observed very focal mainly monopolar (EEG)

and dipolar (MEG) scalp topographies, already supporting the hypothesis that the underlying IEDs were evoked by a brain region with mainly radial orientation. Indeed, this mainly radial and deep candidate region was then confirmed in the FLAIR-MRI and the patient's semiology and corresponded well with the patient's semiology. It is, however, good to know, that the small remaining tangential component of that source, still visible in the MEG, was also localized in close proximity. Furthermore, for an accurate EEG reconstruction without source depth deficit, an accurate head model with individual skull conductivity is needed [9, 19], and in this case study, especially the modeling of the skull burr-holes seems of vital importance [11, 12]. Therefore, we used here the EEG source reconstruction as the possibly best fitting individual target in the optimization of the multi-channel tDCS montage (Fig. 5a). For the first time, we applied this algorithm to a deep and radial target. Surgical intervention could not be recommended in this area due to the proximity to eloquent cortex (Broca), and even if the stimulation of deep target areas is surely more demanding than a superficial one, the application of our optimized multi-channel tDCS could be a non-invasive alternative treatment option with the goal of reducing the number of seizures.

From the results (Fig. 5), we observed that the three main anodal electrodes and the five surrounding circularly arranged cathodes enable a focal stimulation of this deep

⁴ <http://www.sci.utah.edu/cibc-software/scirun.html>

radial target, as the current density distribution (Fig. 5b) and the corresponding indices also showed. The real skull defects are modeled in our scenario, since our FEM forward modeling easily allows the embedding of such skull defects, see also [11, 12]. A next interesting step in the evaluation of optimized multi-channel tDCS montages for the present drug-resistant epilepsy case could be to the burr-holes. Therefore, the same calculation should be repeated with and without modelling of the burr-holes investigate the sensitivity of the tDCS optimization. Furthermore, we will check how different the stimulation is when using the MEG target, since this would in most cases be the target of choice. An improved modeling of the skull compartment with its holes using surface-based tetrahedral FEM or unfitted DG FEM [20] and its effect on the optimization will also be an important further goal. Last but not least, the present work is considered as a case study in presurgical epilepsy diagnosis. Similarly, the performance of source analysis using FEM models in presurgical epilepsy diagnosis was investigated in the past [10, 13, 17]. However, the statistical evaluation of the tDCS effect before and after the stimulation ensures a larger number of patients than one. Therefore, one of the future goals of the present work is to expand the number of patients to assess the statistical significance of the tDCS effects in focal epilepsy.

ACKNOWLEDGMENT

This work was supported by EU project ChildBrain (Marie Curie innovative training network, grant no. 641652), the "Alexander S. Onassis Public Benefit Foundation," the Deutsche Forschungsgemeinschaft, projects WO1425/7-1 and RA2062/1-1 and the DFG priority program SPP1665, project WO1425/5-2. We thank Andreas Wollbrin, Karin Wilken, Hildegard Deitermann, Ute Trompeter, and Harald Kugel for their help with the acquisition of the EEG/MEG/MRI data.

REFERENCES

- [1] M. C. Picot, A. Jaussent, D. Neveu, P. Kahane, A. Crespel, P. Gelisse, et al., "Cost-effectiveness analysis of epilepsy surgery in a controlled cohort of adult patients with intractable partial epilepsy: a 5-year follow-up study," *Epilepsia*, vol. 57, pp. 1669–79, 2016.
- [2] P. Boon, E. De Cock, A. Mertens, E. Trinka, "Neurostimulation for drug-resistant epilepsy: a systematic review of clinical evidence for efficacy, safety, contraindications and predictors for response," *Curr. Opin. Neurol.*, vol. 31(2), pp. 198–210, April 2018.
- [3] F. Fregni, S. Thoma-Souza, M. A. Nitsche, S. D. Freedman, "A controlled clinical trial of cathodal DC polarization in patients with refractory epilepsy," *Epilepsia*, vol. 47, pp. 335–342, 2006.
- [4] M. A. Nitsche and W. Paulus, "Excitability changes induced in the human motor cortex by weak transcranial direct current stimulation," *J. Physiol.*, vol. 527, pp. 3:633–9W, Sep. 2000.
- [5] M. A. Nitsche et al., "Level of action of cathodal DC polarisation induced inhibition of the human motor cortex," *Clin. Neurophysiol.*, vol. 114, pp. 600–4, April 2003.
- [6] A. Baltus, et al., "Optimized auditory transcranial alternating current stimulation improves individual auditory temporal resolution," *Brain Stimulation*, vol. 11(1), pp. 118–124, 2018.
- [7] J. P. Dmochowski, P. Datta, M. Bikson, Y. Su, and L. C. Parra, "Optimized multi-electrode stimulation increases focality and intensity at target," *J. Neural. Eng.*, vol. 8, pp. 1–16, June 2011.
- [8] S. Wagner, M. Burger, C. H. Wolters, "An optimization approach for well-targeted transcranial direct current stimulation," *SIAM J. Appl. Math.*, vol. 76(6), pp. 2154–2174, 2016.
- [9] M. Antonakakis, et al., "The effect of stimulation type, head modeling and combined EEG and MEG on the source reconstruction of the somatosensory P20/N20 component," *Hum. Brain Map.*, First published: August 2019 <https://doi.org/10.1002/hbm.24754>.
- [10] Ü. Aydin, et al., "Combining EEG and MEG for the reconstruction of epileptic activity using a calibrated realistic volume conductor model," *PLoS One*, vol. 9(3), pp. e93154, 2014.
- [11] B. Lanfer, et al., "Influences of skull segmentation inaccuracies on EEG source analysis," *Neuroimage*, vol. 62(1), pp. 418–31 Aug. 2012.
- [12] S. Lau, et al., "Skull defects in finite element head models for source reconstruction from magnetoencephalography signals," *Front. Neurosci.*, vol. 10:141, pp.1–15, 2016.
- [13] Ü. Aydin, et al., "Combined EEG/MEG Can Outperform Single Modality EEG or MEG Source Reconstruction in Presurgical Epilepsy Diagnosis," *PLoS ONE*, vol. 10(3), pp. e0118753, 2015.
- [14] J. K. Rice, C. Rorden, J. S. Little, L. C. Parra, "Subject position affects EEG magnitudes," *Neuroimage* vol. 64, pp. 476–84, 2011. doi: 10.1016/j.neuroimage.2012.09.041.
- [15] M. Antonakakis, et al., "Altered cross-frequency coupling in resting-state MEG after mild traumatic brain injury," *Int. J. Psychophysiol.* April 2016.
- [16] L. Ruthotto, et al., "Diffeomorphic susceptibility artifact correction of diffusion-weighted magnetic resonance images," *Phys. Med. Biol.*, vol. 57(18), pp.5715–5731, 2012.
- [17] Ü. Aydin, S. Rampp, A. Wollbrink, H. Kugel, J. H. Cho, T. R. Knösche, C. Grova, J. Wellmer, C. H. Wolters, "Zoomed MRI guided by combined EEG/MEG source analysis: A multimodal approach for optimizing presurgical epilepsy work-up and its application in a multi-focal epilepsy patient case study," *Brain Topography*, vol. 30(4), pp. :417–433, 2017.
- [18] M. C. Piasra, "New Finite Element Methods for MEG and combined EEG/MEG Forward Problem", PhD thesis, March, 2019.
- [19] J. Vorwerk, et al., "Influence of head tissue conductivity uncertainties on EEG dipole reconstruction," *Front. Neurosci.*, accepted for publication. 2019.
- [20] A. Nüßing, et al., "The Unfitted Dis-continuous Galerkin Method for Solving the EEG Forward Problem," *IEEE Trans Biomed Eng.*, vol. 63(12), pp. 2564–2575, 2016.